論文 / 著書情報
Article / Book Information

Title	Rough Terrain Traveling Method Using an Elastic Telescopic Arm and a Tether
Authors	Toshiya Nagai, Atsushi Ogawa, Hiroyuki Nabae, Koichi Suzumori, Gen Endo
Citation	2022 IEEE/ASME International Conference on Advanced Intelligent Mechatronics (AIM), , ,
Pub. date	2022, 7
Copyright	(c) 2022 IEEE. Personal use of this material is permitted. Permission from IEEE must be obtained for all other uses, in any current or future media, including reprinting/republishing this material for advertising or promotional purposes, creating new collective works, for resale or redistribution to servers or lists, or reuse of any copyrighted component of this work in other works.
DOI	http://dx.doi.org/10.1109/AIM52237.2022.9863408
Note	This file is author (final) version.

Rough Terrain Traveling Method Using an Elastic Telescopic Arm and a Tether

Toshiya Nagai[1], Atsushi Ogawa[1], Hiroyuki Nabae[1], *Member, IEEE*,
Koichi Suzumori[1], *Senior Member, IEEE*, and Gen Endo[1] *Member, IEEE*

***Abstract*— Towing a mobile platform with a tether fixed to the external environment is an effective way to traverse rough terrain. A flexibly bendable telescopic arm that can carry the tether at its arm tip was developed in a previous study. This study is focused on the rough terrain traveling method using a compact elastic telescopic arm installed on a mobile platform. Furthermore, by fusing the linear and bending mechanisms, we developed an elastic telescopic arm that is compact and can perform extension and bending motions on the same body. The results of the arm operation experiment showed that the extension-to-contraction ratio was improved by 16%, and the tip position control accuracy was improved by 70% compared to the previous study. Finally, the effectiveness of the proposed method was demonstrated by a step-climbing experiment, wherein, the step height was more than the wheel diameter of the mobile platform.**

***Index Terms*— Mobile Robots, Control Application in Mechatronics, Modeling and Design of Mechatronic Systems**

I. INTRODUCTION

The use of tethers is effective in improving the rough terrain traveling performance of mobile robots. Teamed robots for exploration and science on steep areas [1] consists of two anchor robots and one mobile robot. Two anchor robots are fixed on the top of a slope, and two tethers attached to the mobile robot are fed out to travel stably on a steep slope. Axel rover [2] is a robot that can separate the front wheels of a 4-wheel drive robot while connected to the tether. The rear wheels are fixed to the ground to feed the tether so that the front wheels can travel independently on a steep slope. The tether-towing-type four-wheeled mobile robot [3] is equipped with a take-up mechanism and travels on a slope while sending out a single tether fixed at the top. However, these methods require the tether to be fixed to the top of the slope or the tether take-up mechanism to be fixed to the top of the slope, which limits the moving range of the robot. Thus, fixing the tether to the external environment remains a problem.

Another method has been reported, wherein, the gripper is thrown out to the external environment such that it gets hooked to a sturdy object; this increases the range of movement by towing with the tether attached to the gripper. Studies on the casting manipulation of grippers [4][5] fix the tether to the external environment by casting. However, these methods have problems such as uncertainty, hazard of casting of the grippers, and difficulty in manufacturing a driving mechanism with a wide range of reduction ratios that can handle both winding and casting.

In this study, we propose a method to fix the tether quasi-statically to the external environment by using a long-reached arm installed on a mobile platform. The arm must be lightweight, have a large extension-to-contraction ratio, and be compact to be mounted on a mobile platform.

The existing lightweight and highly storable arms include spiral zippers [6] and telescopic arms that use convex tapes [7]. These arms are vulnerable to bending moments and are not suitable for horizontal extension and contraction because they cannot support their own weight when they are lengthened. In addition, these arms cannot avoid obstacles in the direction

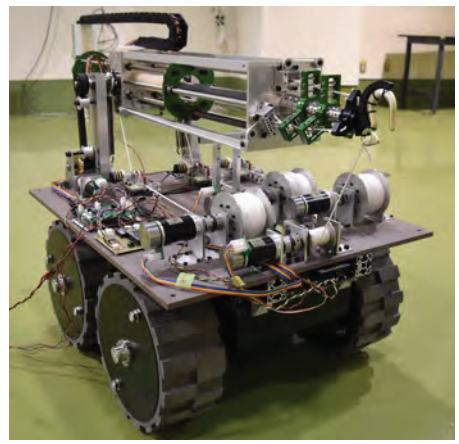

Fig. 1. Mobile robot equipped with elastic telescopic arm

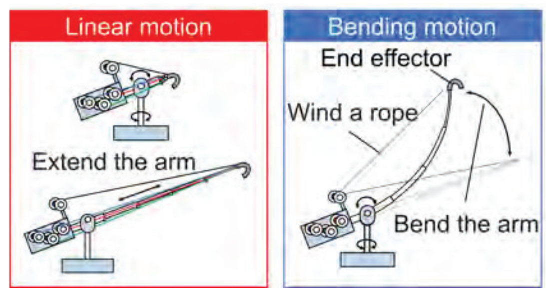

Fig. 2. ETA is compact due to its telescopic structure and can be bent with a rope due to its low arm rigidity.

*Related with the development of telescopic arm mechanism using rope, a part of this work was supported by JAEA Nuclear Energy S&T and Human Resource Development Project through concentrating wisdom under Grant JPJA19P 19210348. This study is based on the results obtained from a project commissioned by the New Energy and Industrial Technology Development Organization (NEDO).

[1]All authors are with the Department of Mechanical Engineering, Tokyo Institute of Technology, Tokyo 152-8550, Japan (e-mail: nagai.t.ah@m.titech.ac.jp; nabae.h.aa@m.titech.ac.jp; suzumori.k.aa @m.titech.ac.jp; endo.g.aa@m.titech.ac.jp)

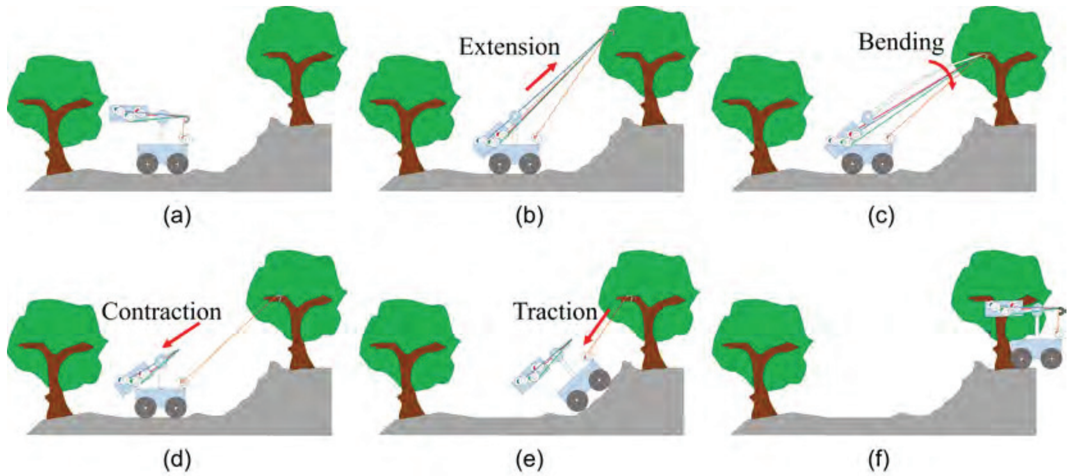

Fig. 3. Traveling method for rough terrain using elastic telescopic arm:
(a) Determination of the target (b) Extension of the arm (c) Control of the tip position and fixing the hook (d) Contraction of the arm (e) Traction by winding rope (f) Traversing on rough terrain

of extension, and their reach to the external environment are limited. Furthermore, because the tip position is controlled by rotation at the base, a highly accurate rotation angle control is required at the base as the arm becomes longer.

To enable a motion other than the linear motion, a bendable telescopic arm named "Elastic Telescopic Arm (ETA)" was proposed by our laboratory [8]. Compared to the conventional telescopic arm, the ETA has elasticity similar to that of a fishing rod. The arm was bent by winding a rope fixed to the arm tip. Hence, the tip position can be precisely controlled even when the arm becomes longer owing to the arm tip being directly actuated by the rope. The prototype was developed in the previous study [9]. In the following, we call this prototype the previous prototype and the new prototype developed in this paper the improved prototype. In previous prototype, the extension and bending mechanisms were separately equipped. When the extension and bending mechanisms were integrated, some mechanical parts for linear and bending motions interfered with each other, and there were units where extension was not possible. A ETA installed on a mobile platforme requires both linear and bending motions to improve the step traverse ability.

In this study, we propose a robot equipped with an ETA and a mobile platform as shown in Fig. 1. As shown in Fig. 2, the ETA requires linear and bending mechanisms that are as compact as possible. Therefore, the improved prototype of ETA that can be installed on a vehicle was developed by integrating the mechanical parts for extension and bending. We also propose a rough terrain traversing method using ETA and its mechanism. In this study, our goal is to demonstrate a series of operations of the arm extension, hook fixing by tip position control, and arm contraction by hardware experiments. Finally, the effectiveness of tethered rough terrain traveling method was demonstrated in a step-climbing experiment. (Note that there are previous studies regarding the method of removing the hook [10] [11], which are not dealt with in this paper.)

The remainder of this paper is organized as follows. Section II proposes a new traveling method for rough terrain using an ETA. Section III describes the basic ideas and working principles of the ETA. Section IV describes the improvements in the mechanical design of the ETA, which includes; a higher extension-to-contraction ratio in comparison to the previous studies, and the integration with the mobile platform. In section V, the motion experiment of the ETA and the improvement of the traveling capability on rough terrain using the ETA are demonstrated, and Section VI concludes the paper.

II. Traveling Method on Rough Terrain Using an Elastic Telescopic Arm

We propose a new traveling method for rough terrain using an ETA. Fig. 3 (a)-(f) present the outline of the proposed method. (a) The hook is roughly positioned towards the target by adjusting the orientation of the vehicle and controlling the root pitch joint of the arm. (b) The arm extends to bring it sufficiently close to the target. (c) The arm is bent by winding the rope attached to the arm tip. The position of the arm tip is directly controlled to attach the hook onto the target. (d) The arm contracts, and the hook is detached from the arm. (e) The tether attached to the hook is wound up, which, results in the vehicle being towed over the rough terrain. (f) After moving over the rough terrain, the hook is detached from the target. Finally, the tether is wound up completely, and the hook is reattached to the arm tip, thus, restoring the initial state.

The proposed method of traveling on rough terrain has the following advantages over the previous methods. First, compared with the previous method using tethers [1]-[3], the proposed method allows the moving vehicle equipped with an ETA to move on rough terrain without using multiple robots. Second, compared to the method of attaching the gripper to a random sturdy object in the external environment by casting [4][5], the hook can be quasi-statically fixed to the external environment by precisely controlling the position of the arm

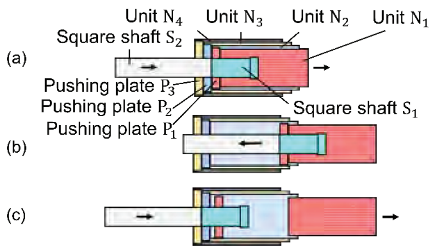

Fig. 4. Stretching method that selects a unit using a square shaft and stretches it with a push plate

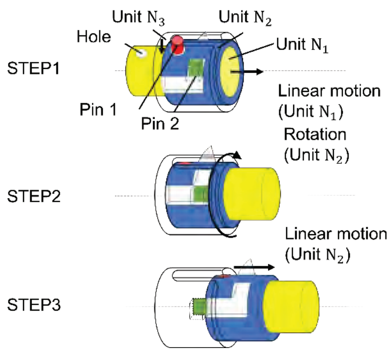

Fig. 5. Concept of constraint mechanism

tip, thus realizing the quasi-static rough terrain traversing. In addition, the traction mechanism needs to only consider the tether winding and does not require a wide reduction to generate enough force to cast the gripper. Finally, compared with the conventional straight-extension arm [6][7], the ETA can be bent by applying tension to the rope at the end of the arm to avoid obstacles in the direction of extension and reach the target. The space robot REX-J [12] has a method with similar movement, but the arm can only extend straight and cannot avoid obstacles in the direction of extension.

III. MECHANISM AND OPERATION OF ELASTIC TELESCOPIC ARM

In this chapter, the principles of extension and bending motions of the ETA are explained. The principle of operation is based on the previous studies [8][9].

A. Outline of the linear mechanism

Figure 4 shows the basic operation of the linear mechanism. Fig. 4 (a)-(c) show the procedure for the extending unit N_1. Select the unit N_i to be extended in succession with the pushing plate P_i, and extend them from the tip in an orderly manner. The square shafts S_1 and S_2 can move linearly in the direction of extension, and only the tip shaft S_1 can rotate. By controlling the position of the square shaft and the rotation angle around the axis, the unit and the push plate are selected, and the target unit is extruded. The processes from (a)-(c) are described below.

(a) Adjust the position of the square shaft and align the left end of the corresponding push plate P_1 with unit N_1 to be extended and the left end of square shaft S_1. Rotate square shaft S_1 to rotate push plate P_1 and unit N_1.

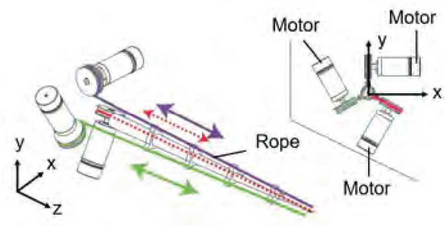

Fig. 6. Arrangement of bending motors

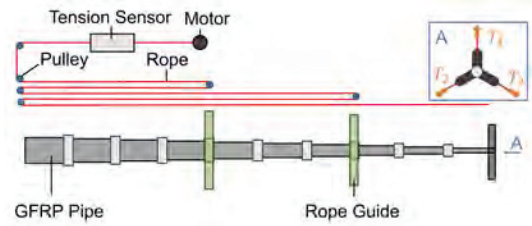

Fig. 7. A large bending moment is generated toward the base of the arm by arranging the rope folded back.

(b) The square shaft is moved linearly, unit N_1 and push plate P_1 are pushed out, and the arm is extended.

(c) After extending unit N_1, align the left ends of push plate P_2 with square shaft S_1 to extend unit N_2. At this time, unit N_1 remains in the stretched state.

By repeating the processes from (a)-(c), units N_2 and N_3 can be extended. By repeating this process, it is possible to extend all the units with a reciprocating motion of one unit. The details of the selection method of the push plate and the units in the linear mechanism are described in a previous study [9].

When the target unit is selected for extension, if the friction between the units is large, other unselected units may also be extended. In addition, when the arm was bent, the rope attached to the arm tip exerted a force in the direction of contraction. Thus, it is necessary to prevent the arm from contraction. Fig. 5 shows the mechanism to constrain these unintended motions; the process from STEP1 to STEP3 shows the extension of unit N_1 to N_2. The constraint mechanism uses two types of pin to constrain the linear and rotational movements of the units. Pin 1, which is fixed in unit N_2, stops unit N_2 from rotating against unit N_3. Pin 2, which is fixed in unit N_3, stops unit N_2 from extending against unit N_3. The details of the release method for the constraint mechanism are described in our previous study [9].

The arm can be extended sequentially by repeatedly releasing the constraint mechanism. This procedure should be reversed when contracting the arm. Pin 1 is mechanically designed to be removed from the hole when a certain force is applied.

B. Outline of the bending mechanism

The motor arrangement of the tendon drive unit is shown in Fig. 6. The coordinate system is defined as a right-handed system with the longitudinal section of the arm in the z-direction and the vertical upward section in the y-direction. This drive system allows the arm to bend in the xy-plane

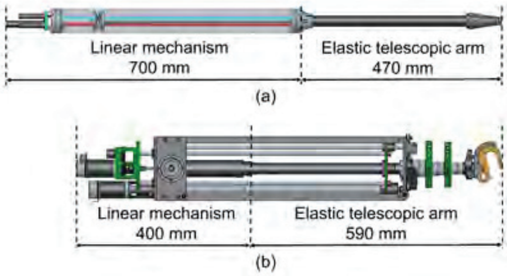

Fig. 8. Comparison with conventional linear mechanism (a) previous prototype (b) improved prototype

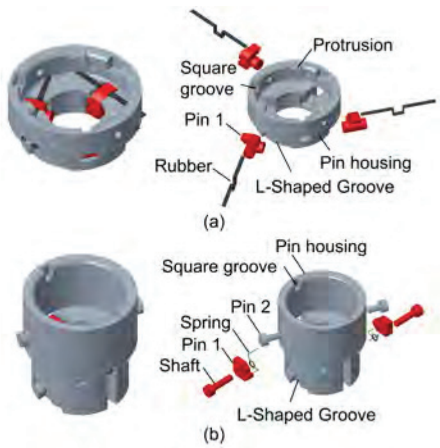

Fig. 9. Improvement of the constraint mechanism (a) previous prototype (b) improved prototype

owing to the resultant force of the three rope tensions. The rope pathway adopted from a previous study [13][14] is shown in Fig. 7. Tension was applied by reciprocating the rope, using a rope guide fixed to the outside of the arm, to all the pulleys through which the rope passes, and tension was applied at multiple positions in the structure. Therefore, the bending moment gradually increased toward the base of the arm; therefore, the bending motion of the entire arm is possible.

IV. DEVELOPMENT OF PROTOTYPE

Regarding the previous prototype of the ETA, the problems encountered when mounting it on a mobile platform are listed below.

- The linear mechanism in the longitudinal direction is large in size.
- The strength of the constraint mechanism is low, and it cannot withstand the contraction force during contraction and bending moment during bending of the arm.
- The rope guide and constraint mechanism interfere with each other, and the extension and bending operations cannot be performed continuously.

Therefore, in this chapter, we report the improvements in the linear and constraint mechanisms in the improved prototype and compare them with the previous prototype. In addition, we describe a prototype that integrates the improved prototype of ETA and the mobile platform.

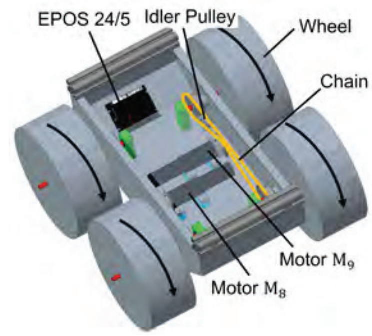

Fig. 10. Overview of mobile platform

TABLE I. Specifications of mobile platform (Motors M_8 and M_9 : 335804, Maxon Motor)

Size (L × W × H) [mm]	630 × 580 × 290
Weight (with battery) [kg]	18
Wheel Diameter [mm]	290
Power of the motors M_8 and M_9 [W]	70
Reduction of the motors M_8 and M_9	257 : 1

A. Improvement of elastic telescopic arm

Figure 8 shows an overview of the developed linear mechanism. As shown in (a), in the previous prototype, a linear mechanism for extending the ETA is attached at the end of the ETA, and the total size of the mechanism is 1170 mm in the longitudinal direction with the arm in contracted state. In the improved prototype, the linear mechanism and ETA were arranged in parallel to reduce the size in the longitudinal direction. As a result, the total length of the ETA and the linear mechanism can be reduced to 990 mm, as shown in (b).

Figure 9 shows a comparison of the constraint mechanism with the previous prototype. The constraint mechanism of the previous prototype comprises a pin housing, pin 1, and a band-shaped rubber. Owing to the complicated structures and poor machinability, the pin housing and pin 1 were created by the optical 3D printing and metal 3D printing, respectively. However, the pin housing was damaged because it could not withstand the axial compressive force and bending moment during bending. In addition, the tension in the band-shaped rubber, that gives an inward rotation force to pin 1, decreased with each use; thereby, decreasing the rotational force applied to pin 1. Therefore, the projection of the pin housing was divided using pin 2. By separating pin 1 from the shaft, the shapes of the pin housing and pin 1 were changed to be suitable machining. As a result, the rigidity of the pin housing increased. In addition, the band-shaped rubber was replaced by a coiled spring so that the rotational force applied to pin 1 was constant.

B. Mobile platform

The details of mobile platform are presented in Fig. 10 and listed in Table I. The front and rear wheels are connected by chains, and motors M_8 and M_9 drive the left and right wheels, respectively, which enables the mobile vehicle to move forward, backward, and a spin turn by the velocity control of the motors. Two motor drivers (EPOS 24/5 and Maxon Motor)

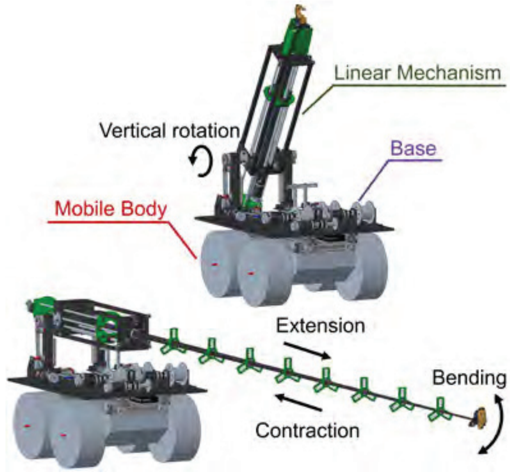

Fig. 11. Structure of the improved prototype equipped with elastic telescopic arm

TABLE II. Specifications of the improved prototype (Motors M_1 to M_7 : 434982, Maxon Motor)

Size (L × W × H) [mm]	940 × 600 × 650
Weight (with battery) [kg]	50
Power of the motors M_1 to M_7 [W]	70
Reduction of the motors M_1 to M_7	156 : 1

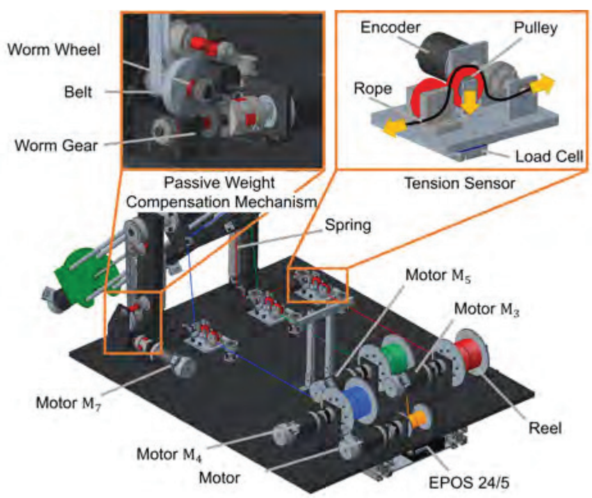

Fig. 12. The base is equipped with a passive weight mechanism and a tension sensor for bending rope.

and a battery were installed inside the mobile vehicle to drive motors M_8 and M_9.

C. Integration of the improved prototype and mobile platform

The details of the robot that integrates an ETA are presented in Fig. 11 and listed in Table II. The robot consists of an ETA, a linear mechanism, a base, and a mobile platform. The robot can rotate the pitch axis of the arm, extend and contract the arm, bend the arm, and travel.

The details of the base are presented in Fig. 12. Motors M_3, M_4, and M_5 are equipped with reels, which is used for winding up the rope to realize the bending motion of the arm. The rope tension was measured by a tension sensor consisting of three pulleys and a load cell (MCDW-50L, Toyo Sokki). Motor M_6 changes the traction tension according to the slope by controlling the current. Motor M_7 rotates the arm and the linear mechanism around the pitch axis via a worm gear and belt. It is equipped with a gravity compensation mechanism [15] that compensates for the rotational torque around the pitch axis caused by its own weight so that the belt does not skip the teeth.

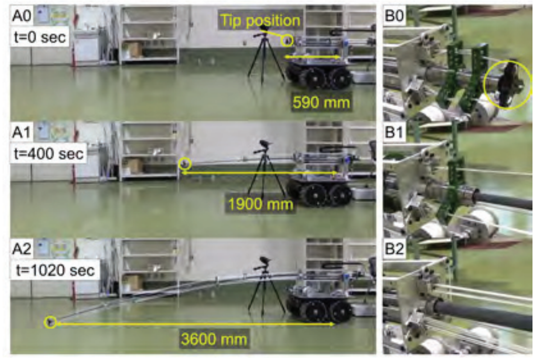

Fig. 13. The arm succeeded in extending from 590 mm to 3600 mm.

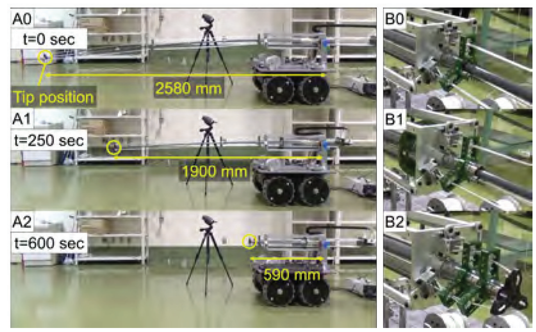

Fig. 14. The arm succeeded in constracting from 2580 mm to 590 mm.

V. EXPERIMENTS

In this section, we report the performance of the linear and bending motions of the improved ETA. As a measure of performance of linear motion, we measured the change in the length of the arm. To evaluate the bending motion, we measured the tip-position accuracy of the arm. The performance results are compared with those of the previous prototype. Finally, the effectiveness of the proposed method was verified by conducting a step-traversing experiment.

A. Extension and contraction experiment

Figure 13 shows the results of the extension experiment. The numbers indicate the time history. Two video cameras were used for filming, and the figures taken by each camera are represented by A and B. As shown in A0 to A2, the arm was successfully extended from 1 unit to 10 units, from 590 mm to 3600 mm, with a stretch ratio of approximately 6:1. As shown in B0 to B2, it was confirmed that the arm could be extended without any interference between the rope guide and

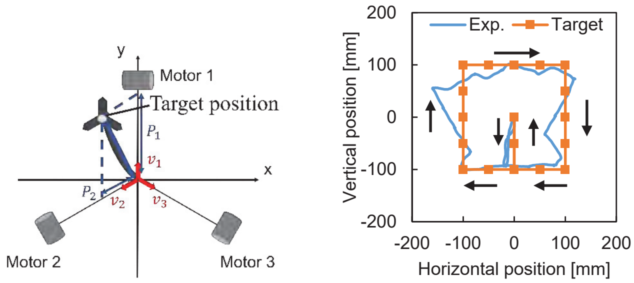

(a) (b)

Fig. 15. Result of tip control experiment
(a) Coordinate of tip position (b) Trajectory of tip position

TABLE III. Tip position accuracy during flexion operation

	previous	improved
Average absolute error x [mm]	78	17
Average absolute error y [mm]	37	15
Average absolute error x by arm length [%]	2.3	0.51
Average absolute error y by arm length [%]	1.1	0.43

the constraint mechanism by sending out the rope during the extension.

Figure 14 shows the results of the contraction experiment. The numbers indicate the time history. As shown in A0 to A2, the arms successfully contracted from 6 units to 1 unit, from 2580 mm to 590 mm, with an expansion-to-contraction ratio of 4.4:1. In addition, as shown in B0 to B2, the contraction was achieved without any interference between the rope guide and constraint mechanism by reeling in the rope during contraction.

B. Bending experiment

A bending motion experiment was performed on the improved prototype, and the accuracy of the tip position control was compared with that of the previous prototype. We also compared the resolution of the tip position by the rope amount control with that by rotation at the base.

Figure 15a shows the coordinates of the arm tip position control. The rope in the v_1 direction is driven by motor M_4, the rope in the v_2 direction by motor M_5, and the rope in the v_3 direction by motor M_6. The x-axis is horizontal and the y-axis is vertical, with the origin at the tip of the arm when no rope tension is applied, and the coordinates of the tip position are represented by p.

Bending experiments were conducted with the arm extended to 3600 mm. The origin was set at a state where all the rope tensions were 0 N. The control command range was 200 mm in both the x and y directions, and the tip position was specified to draw a square in the clockwise direction. The trajectory of the tip position under the rope winding amount control is shown in Fig. 15b. Table III shows a comparison of the average absolute error, average absolute error rate normalized by the control command range, and average absolute error rate normalized by the arm length. The results show that the error rate of the improved prototype is lower than that of the previous prototype for all items.

In this experiment, the resolution of the tip position control

TABLE IV. Comparison between previous prototype and improved prototype

	previous	improved
Number of units	10	10
Length per unit [mm]	400	400
Total length of contracted arm and LM* [mm]	1170	990
Total length of extended arm and LM* [mm]	4040	4000
Weight [kg]	7.0	8.5
Absolute error x by bending [mm]	78	17
Absolute error y by bending [mm]	37	15

* LM: linear mechanism

was 50 mm, which is equivalent to rotation of the robot by 0.80 ° and difficult to achieve on rough terrain. In addition, the arm was expected to vibrate when the robot was rotated. Therefore, the tip position control method by bending the ETA is more suitable than the tip position control method based on robot rotation.

C. Comparison between previous prototype and improved prototype

Table IV lists the results of the experiments. Although the total arm length of the improved prototype was reduced by 17%, its maximum extension length was equivalent to that of the previous prototype owing to its large extension-to-contraction ratio. In addition, the error of the tip position control was reduced by 78% in the x-axis direction and 59% in the y-axis direction compared to the previous prototype.

D. Step climbing experiment

We conducted a series of experiments on climbing a step using tether towing. A 300 mm step was used, and the step height was 103% of the wheel diameter of 290 mm. The hook was fixed to the aluminum frame, and the traction tension gradually increased when the tension was insufficient.

The result of experiment is shown in Fig. 16. The numbers indicate the time history. 0 to 2 shows the process of extending the arm. 3 shows the arm extension process, in which the arm is rotated in the direction of the pitch, the arm is bent according to the extent of rope winding, and the hook is fixed to the external environment. 3 to 5 show the process of contracting the extended arm. 6 to 7 show the process of climbing the step. 6 shows that vehicle is lifted up by traction, and 7 shows that step climbing is completed. Using the ETA, we were able to quasi-statically fix the hook to the external environment and climb the step by traction with a rope.

In addition, to confirm the improvement in the running performance by traction with a tether, we conducted an experiment on step climbing. In general, it is impossible for a moving vehicle to traverse steps that exceed 100% of the wheel diameter. In this study, a step of 155% of the wheel diameter of 290 mm was climbed by a mobile platform equipped with the newly developed ETA; thus, achieving what was assumed to be impossible for a mobile vehicle alone.

VI. CONCLUSION

In this study, we proposed a traveling method for a mobile platform on rough terrain using an ETA to improve its running

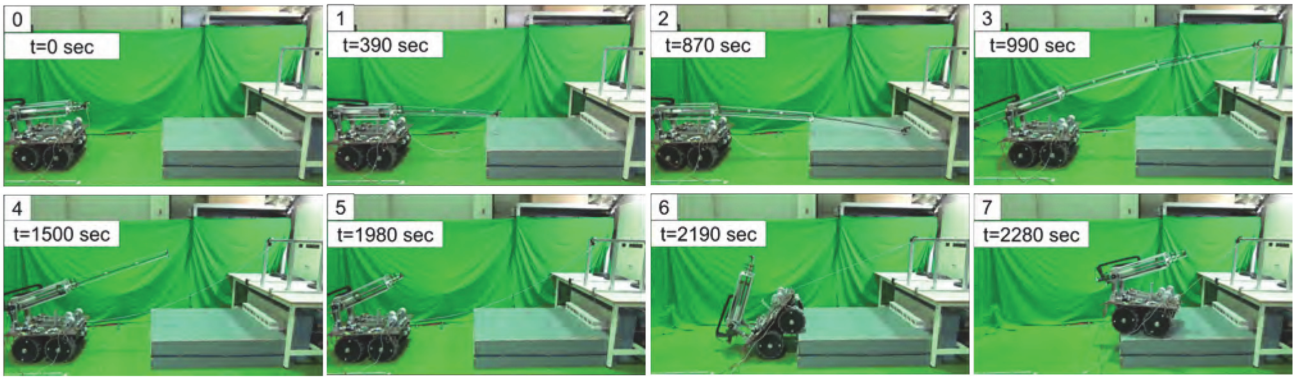

Fig. 16. Traversing experiment on rough terrain by a series of operations: The robot succeeded in traversing steps higher than the wheel diameter.

performance. In the linear motion of the arm, the arm was successfully extended from 590 mm to 3600 mm and contracted from 2580 mm to 590 mm. Furthermore, it was possible to perform an extension operation with a higher extension-to-contraction ratio in the improved prototype when compared to the previous prototype. In addition, the position of the arm tip was controlled by bending the arm. The results showed that the controllability of the tip position was improved.

Finally, a step-climbing experiment was conducted using a prototype that integrated an ETA and a mobile platform. The effectiveness of the proposed rough terrain traveling method was demonstrated by performing a series of operations such as arm extension, bending, contraction, and tethered traction. In addition, we achieved a step climbing of 155% of the wheel diameter, which is assumed to be impossible to traverse with a moving vehicle alone. As a result, it was confirmed that the performance of traveling on rough terrain was improved by mounting an ETA and traction.

However, the residual problem, that is the push plate of the extension and contraction mechanism and the end of the pipe being damaged owing to an excessive load in the contraction operation after the 7 units, is because the frictional force between the units increases as the arm becomes longer, and the contraction force required for contraction also increases. In the future, we plan to improve the strength of the push plate and pipe ends to realize the contraction operation after the 7 units.

ACKNOWLEDGMENT

Related with the development of telescopic arm mechanism using rope, a part of this work was supported by JAEA Nuclear Energy S&T and Human Resource Development Project through concentrating wisdom under Grant JPJA19P 19210348. This study is based on the results obtained from a project commissioned by the New Energy and Industrial Technology Development Organization (NEDO).

REFERENCES

[1] T. Huntsberger, A. Stroupe, H. Aghazarian, M. Garrett, P. Younse, and M. Powell, "Tressa: Teamed robots for exploration and science on steep areas," *Journal of Field Robotics*, vol. 24, no. 11-12, pp. 1015–1031, 2007.

[2] I. A. Nesnas, J. B. Matthews, P. Abad-Manterola, J. W. Burdick, J. A. Edlund, J. C. Morrison, R. D. Peters, M. M. Tanner, R. N. Miyake, B. S. Solish, *et al.*, "Axel and duaxel rovers for the sustainable exploration of extreme terrains," *Journal of Field Robotics*, vol. 29, no. 4, pp. 663–685, 2012.

[3] K. Nagatani, S. Tatano, K. Ikeda, A. Watanabe, and M. Kuri, "Design and development of a tethered mobile robot to traverse on steep slope based on an analysis of its slippage and turnover," in *2017 IEEE/RSJ International Conference on Intelligent Robots and Systems (IROS)*, 2017, pp. 2637–2642.

[4] A. Fagiolini, F. A. W. Belo, M. G. Catalano, F. Bonomo, S. Alicino, and A. Bicchi, "Design and control of a novel 3d casting manipulator," in *2010 IEEE International Conference on Robotics and Automation*, 2010, pp. 4169–4174.

[5] H. Arisumi, K. Yokoi, and K. Komoriya, "Casting manipulation-midair control of a gripper by impulsive force," *IEEE transactions on robotics*, vol. 24, no. 2, pp. 402–415, 2008.

[6] F. Collins and M. Yim, "Design of a spherical robot arm with the spiral zipper prismatic joint," in *2016 IEEE International Conference on Robotics and Automation (ICRA)*, 2016, pp. 2137–2143.

[7] J. Zhang, A. Song, X. Xu, and W. Lu, "A rigid and flexible structures combined deployable boom for space exploration," in *2016 IEEE/RSJ International Conference on Intelligent Robots and Systems (IROS)*, 2016, pp. 2920–2926.

[8] T. Fujioka, G. Endo, K. Suzumori, and H. Nabae, "Proposal of tendon-driven elastic telescopic arm and initial bending experiment," in *2017 IEEE/SICE International Symposium on System Integration (SII)*, 2017, pp. 164–169.

[9] A. Ogawa, T. Fujioka, H. Nabae, K. Suzumori, and G. Endo, "Tendon-driven elastic telescopic arm -integration of linear motion and bending motion-," in *2020 IEEE/SICE International Symposium on System Integration (SII)*, 2020, pp. 1328–1334.

[10] N. Asano, H. Nakamoto, T. Hagiwara, and S. Hirose, "Tethered detachable hook for the spiderman locomotion (design of the hook and its launching winch)," in *Field and Service Robotics*. Springer, 2010, pp. 25–34.

[11] T. Bridgwater, G. Griffiths, A. Winfield, and T. Pipe, "A novel design for a robot grappling hook for use in a nuclear cave environment," *IFAC-PapersOnLine*, vol. 49, no. 21, pp. 288–293, 2016.

[12] M. Oda, M. Yoshii, H. Nakanishi, H. Kato, A. Ueta, S. Suzuki, and M. Yamazumi, "Development of an astronaut support robot and its precursor rex-j, to be tested on the international space station," in *International Symposium on Artificial Intelligence, Robotics and Automation in Space (i-SAIRAS)*, 2012.

[13] K. Oliver-Butler, J. Till, and C. Rucker, "Continuum robot stiffness under external loads and prescribed tendon displacements," *IEEE Transactions on Robotics*, vol. 35, no. 2, pp. 403–419, 2019.

[14] M. C. Lastinger, S. Verma, A. D. Kapadia, and I. D. Walker, "Tree: A variable topology, branching continuum robot," in *2019 International Conference on Robotics and Automation (ICRA)*, 2019, pp. 5365–5371.

[15] G. Endo, H. Yamada, A. Yajima, M. Ogata, and S. Hirose, "A passive weight compensation mechanism with a non-circular pulley and a spring," in *2010 IEEE International Conference on Robotics and Automation*, 2010, pp. 3843–3848.